#1

Antenna 3 Efficiency Measurements

Dick Plambeck
31 March 1986

summary

In February the panels on antenna 3 were adjusted to reduce the rms error of the surface to 0.002 inches (50 microns). Observations of Jupiter and Venus were then used to measure the antenna aperture efficiency at 80, 95, and 110 GHz, with and without Jerry Hudson's dielectric lens installed in front of the feed horn. The aperture efficiency was roughly 55–60% without the lens, 65–70% with it; the lens appears to add less than 2 K to the system temperature.

This memo describes the panel adjustment procedure and the aperture efficiency measurements.

panel adjustment

The surface of the antenna was measured holographically – that is, the interferometer was used to map the amplitude *and* phase of the antenna beam pattern; the beam pattern was then Fourier transformed to produce maps of the electric field amplitude and phase across the aperture. High and low spots on the antenna surface show up as phase variations across the aperture.

The beam pattern was mapped with program ZIP, using the 85.27 GHz transmitter at the Hat Creek Rim lookout tower. ZIP samples the correlator output of the old wideband receiver; it scans antenna 3 across the transmitter while antenna 1 or 2, serving as a reference antenna, is pointed straight at the transmitter. Normally the beam pattern was sampled on a 63 × 63 grid, with cells spaced by 1.5 arcminutes. About 2 hours were required to sample this grid.

Program BMAP was used to Fourier transform the beam pattern in order to produce maps of the voltage and phase across the antenna aperture; these maps have a resolution of approximately 5 inches on the antenna surface. Slight pointing errors on the transmitter lead to linear phase gradients across the aperture, while defocussing leads to a quadratic phase error; BMAP removes these terms with a least squares fit before plotting the phase. If the subreflector is displaced laterally, a cubic phase error (coma) appears; the present version of BMAP does not attempt to fit this term.

Figure 1 shows a plot of the phase across the antenna before any panel adjustments were made. The phase has been converted to the equivalent surface error in units of .001 inch; the rms error is .0062 inches. Each panel is attached to the backup structure with 6 adjustment screws (with 16 threads per inch pitch). These screws – except those along the inner edge of the inner panels, which are almost impossible to reach – were

adjusted to improve the antenna surface. The first set of panel adjustments, done 22-25 November 1985, reduced the rms error to .0024 inches; a second set of adjustments, done 20-22 February 1986, brought the rms error down to .0018 inches (Figure 2). The numbers actually used to compute the rms error are shown in Figure 3; points within 1 resolution element (5 inches) of the feed legs, central blockage, or edge of the dish have been discarded. All points were given uniform weight in calculating the rms.

Surface errors which occur on a scale smaller than 5 inches are not visible in our maps. Presumably, surface roughness on this scale is attributable primarily to the ridges left on the surface of the panels when they were machined; the rms error due to these ridges is approximately 0.0008 inches (see Figure 4). Thus, the true rms error of the surface is approximately 0.002 inches (50 microns). An rms surface error ϵ degrades the antenna aperture efficiency by a factor $f = e^{-(4\pi\epsilon/\lambda)^2}$; for antenna 3, $f = 0.94$ at 115 GHz and 0.79 at 230 GHz.

The beam patterns before and after adjustment are shown in Figure 5. A halftone representation of the extended beam pattern is shown in Figure 6; diffraction spikes due to the feed leg blockage are clearly visible.

the dielectric lens

For some of the aperture efficiency measurements, a Teflon lens designed by Jerry Hudson was installed in front of the feed horn. The lens reduces spillover past the subreflector and produces a more uniform illumination of the dish, thus improving the aperture efficiency. The lens was mounted inside the receiver enclosure with its flat surface towards the dewar, 6.5 inches in front of the dewar wall. The subreflector must be refocused when the lens is installed; the in/out focus setting should be reduced by approximately 200–300 octal units, which moves the subreflector approximately 0.080 inches farther away from the dish. (According to measurements which Jim and I made, decreasing the in/out focus by 2000 octal units moves the subreflector away from the dish by 0.52 inches.)

Figures 7 and 8 compare the antenna beam patterns and aperture illuminations measured with and without the lens.

We have not made a direct measurement of the insertion loss of the lens. Antenna dipping measurements (see section (4) below) made with and without the lens showed, however, that the system temperature at zenith increased by less than 2 K when the lens was installed, which indicates that its loss is less than 1%.

aperture efficiency measurements

Observations of Jupiter and Venus were used to measure the antenna aperture efficiency at 80, 95, and 110 GHz. The observations were done on 24 Feb 86 in clear, calm weather. All measurements were made during the day, with the sun shining on the antenna. The

following procedure was used:

(1) *Focus.* The antenna focus was optimized by making a series of 3 × 3 pointing crosses on Jupiter or Venus (using program QPT), each at a different subreflector in/out position. Focus curves obtained in this way are shown in Figure 9. The focus was set to 4200 (octal) for measurements without the lens and to 3640 (octal) for measurements with the lens. The optimum focus setting was measured again late in the afternoon when the lens was removed, and was found to be 4040 (octal). The best focus for the remote transmitter is approximately 100 octal units less than that for astronomical sources; the transmitter is located just 5 km from the observatory, and thus is not truly in the far field of the antenna.

(2) *Pointing.* Program QPT was used to measure the pointing offset just prior to each switched power observation on a planet. The pointing was found to be quite stable throughout the day (see Table 2, column 5).

(3) *Switched power observations.* Program SWP was used to make total power position-switched measurements. SWP samples the zero lag channel of the digital correlator with subroutine LEVELS; the correlator was set up in mode 4, with 40 MHz bandwidths. SWP uses the following observing strategy:

(a) with antenna pointed 10 arcminutes off source, receiver looking at sky, set correlator clipping levels

(b) measure total power on AMB and COLD flaps, and ZERO offset with equalizer IF amplifier turned off; note elevation of source

(c) point ON-source; offset pointing by corrections determined in step (2); wait 8 seconds for tracking to stabilize before measuring total power

(d) point 10 arcminutes OFF-source, in azimuth; measure total power

(e) repeat calibration cycle after every 10 ON-OFF measurements

An integration time of 2 seconds was used for each total power measurement; normally, data was taken for about 20 on–off cycles. The planet antenna temperature was calculated as:

$$T_A = \frac{T_{amb} - T_{cold}}{\langle AMB \rangle - \langle COLD \rangle} \langle ON - OFF \rangle$$

where T_{amb} and T_{cold} are the physical temperatures of the ambient and cold flaps, as measured with thermistors mounted on or near the flaps. For these observations, T_{cold} was 35 K; T_{amb}, 294 K.

(4) *Antenna dipping.* Program DIP was used to measure the receiver total power (again, with the digital correlator) at 11 different antenna elevations, in steps of 0.1 airmass,

from 1 to 2 airmasses [airmass = 1/sin(elev)]. COLD, AMB, and ZERO are measured before and after the antenna dip. The double sideband receiver and system temperatures are given by:

$$T_{rcvr} = \frac{COLD - OFF}{AMB - COLD}(T_{amb} - T_{cold}) - T_{cold}$$

$$T_{sys} = \frac{SKY - OFF}{AMB - COLD}(T_{amb} - T_{cold})$$

The system temperature is expected to be a function of airmass A of the form:

$$T_{sys} = T_{rcvr} + T_{tel} + T_{bg}e^{-\tau A} + T_{atm}\left(1 - e^{-\tau A}\right)$$

where T_{tel} represents antenna losses which are terminated at ambient temperature, T_{bg} is the 3 K cosmic background radiation, and T_{atm} is the effective temperature of the absorbing layers in the atmosphere. According to atmospheric models (cf. Ulich 1980, Astrophysical Letters, **21**, 21) $T_{atm} \approx 0.94\, T_{outdoor}$.

Figures 10–12 show typical dipping curves at 80, 95, and 110 GHz. The solid curves are fits to the data obtained if one assumes $T_{atm} = 270K$. The atmospheric opacities derived are as follows:

ν	τ_{fit}	τ_{theor}
80 GHz	0.170 ± 0.015	0.180
95 GHz	0.175 ± 0.015	0.178
110 GHz	0.254 ± 0.025	0.255

Uncertainties in the opacities were calculated by allowing T_{atm} to vary from 250 to 290 K. Theoretical opacities were calculated with program [plambeck.atten]atat0, and are appropriate for a 1 km high site with 15 mm precipitable water. Note that such a high water vapor content is quite uncharacteristic of Hat Creek in February; 4 to 8 mm precipitable water is typical.

When extrapolated to zero airmasses, the system temperature is found to be 13 to 18 K higher than the receiver temperature, which implies that $T_{tel} \approx$10–15 K, corresponding to a telescope loss of 3–5%. Presumably this loss is attributable to scattering by the feedlegs or subreflector of ground radiation into the receiver, to ohmic losses in the panels, and to losses in the Teflon dewar window or receiver cover.

A log of the observations is given in Table 1.

computation of the aperture efficiency

The antenna aperture efficiency is given by:

$$\eta_A = \frac{2kT_A e^{\tau A} F_D}{A_g S} = \frac{94.56}{(S/T_A e^{\tau A} F_D)\ (Jy/K)}$$

Here $T_A e^{\tau A}$ is the observed planet antenna temperature corrected for atmospheric extinction, F_D is the disk resolution factor, A_g is the geometrical area of the antenna, and S is the planet flux density. The disk resolution factor F_D corrects for the fact that the planet is not a point source. It is given by (Baars 1973, IEEE Transactions, **AP-21**, 461):

$$F_D = \frac{x^2}{1 - exp(-x^2)}$$

where $x = R/0.6\ \theta_{\rm FWHM}$; R is the planet semidiameter and $\theta_{\rm FWHM}$ is the half power beamwidth of the antenna. The planet flux density S is given by:

$$S = \frac{2h\nu^3\Omega}{c^2} \frac{1}{exp(h\nu/kT_B) - 1}$$

$$\Omega(\text{steradians}) = \text{solid angle of planetary disk} = 7.384 \times 10^{-11} R_{maj}('')R_{min}('')$$

The brightness temperatures T_B of Jupiter and Venus were assumed to be 179 K and 358 K, respectively (Ulich et al. 1980, IEEE Transactions, **AP-28**, 367); the planet semidiameters on 24 Feb 86 were $16.39'' \times 15.39''$ for Jupiter, $4.94'' \times 4.94''$ for Venus.

Table 2 summarizes the aperture efficiency calculations. The uncertainties listed for the aperture efficiencies are due principally to uncertainties in the atmospheric extinction corrections.

The aperture efficiency measurements are plotted versus frequency in Figure 13. There is a particularly large scatter in the measurements made with the dielectric lens installed. This scatter may possibly be caused by small movements of the subreflector (due to sag or to the feed legs warping in the sun). If the aperture is illuminated nearly uniformly, as it is when the lens is installed, then the forward gain is likely to drop more noticeably if the subreflector moves slightly off–axis than if the illumination is strongly tapered, as it is when the lens is not installed.

The falloff in efficiency at higher frequencies might also be caused by subreflector movement, or might occur because the aperture illumination is not ideal at the high end of

the band; alternatively, it may indicate that the planet temperatures which we assumed (which are based on measurements at 86.1 GHz) are not appropriate at 110 GHz. The falloff in efficiency is unlikely to be caused by surface errors on the antenna itself. The smooth curves drawn through the measured points suggest that the aperture efficiency is roughly 55%–60% without the lens, 65%–70% with the lens installed.

Table 1. Log of Observations

UT	freq (GHz)	planet	lens	daz, del (arcmin)	airmass	T_A (K)
18:11	80	Jupiter	no	.35, .00	1.90	3.10 (.03)
18:48	95	Jupiter	no	.40, .05	1.74	4.14 (.05)
19:31	110	Jupiter	no	.40, -.15	1.66	4.32 (.03)
20:51	110	Jupiter	yes	.20, -.05	1.71	5.09 (.05)
21:30	110	Venus	yes	.18, -.12	1.53	1.05 (.02)
22:02	95	Jupiter	yes	.05, -.05	2.00	4.34 (.06)
22:14	95	Venus	yes	.05, -.05	1.63	1.10 (.05)
22:41	80	Jupiter	yes	-.05, .15	2.35	3.25 (.04)
22:55	80	Venus	yes	-.05, .15	1.80	0.79 (.02)
23:56	80	Venus	no	-.25, -.20	2.32	0.55 (.02)

Table 2. Aperture efficiency calculations

freq (GHz)	planet	flux (Jy)	lens	beamwidth (arcmin)	F_D	$T_A \exp(\tau A)$ (K)	eta
80	Jupiter	648	no	2.65	1.014	4.28 (.12)	0.63 (.02)
80	Jupiter	648	yes	2.35	1.018	4.85 (.18)	0.72 (.03)
80	Venus	126	no	2.65	1.00	0.82 (.04)	0.62 (.03)
80	Venus	126	yes	2.35	1.00	1.07 (.04)	0.80 (.03)
95	Jupiter	913	no	2.25	1.019	5.61 (.16)	0.59 (.02)
95	Jupiter	913	yes	2.00	1.025	6.16 (.19)	0.65 (.02)
95	Venus	178	yes	2.00	1.00	1.46 (.06)	0.78 (.03)
110	Jupiter	1222	no	1.95	1.026	6.59 (.27)	0.52 (.02)
110	Jupiter	1222	yes	1.70	1.034	7.86 (.34)	0.63 (.03)
110	Venus	238	yes	1.70	1.00	1.55 (.06)	0.62 (.02)

Note: the antenna beamwidths indicated here were scaled from those measured at 85.27 GHz on the remote transmitter (see Figure 7).

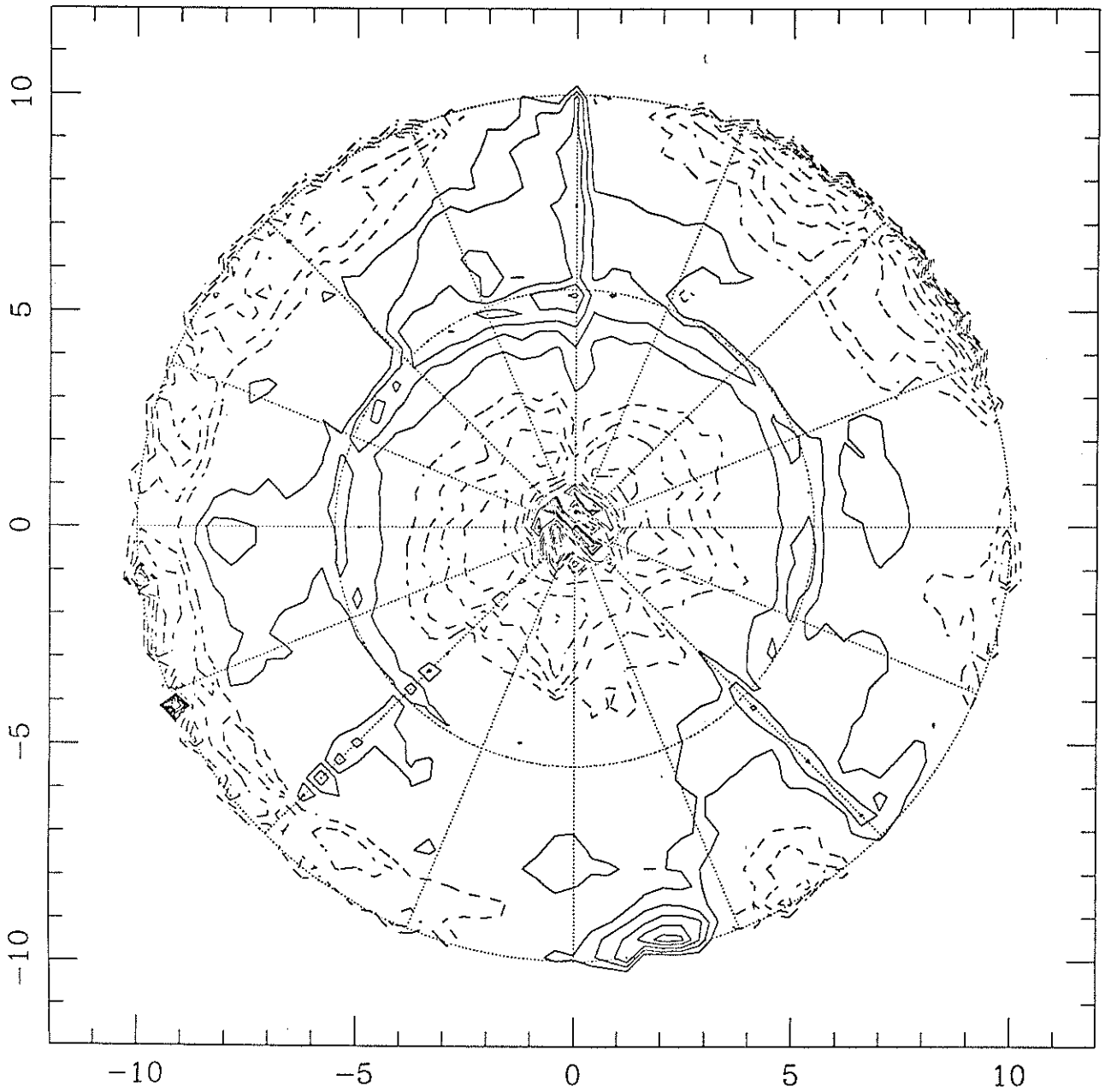

bmap31.20n;1
ANTEN: 31

20−NOV−85
2:21 UT

IN/OUT FOCUS: 0
UP/DWN FOCUS: 0

CONTOURS:
−36.0 TO 36.0
INTERVAL 3.6

AFTER SUBTRACTING:
5.50 +0.84 X +
−0.07 Y −0.14 RSQ

RMS: 0.0062 INCHES

Figure 1. Aperture phase measured before panel adjustments, 20 Nov 1985. Phase has been converted into the equivalent surface error in units of .001 inch; the contour interval is .0036 inches. In this view, we are looking from the subreflector toward the dish. Positive contours represent high spots on the dish; negative contours, low spots.

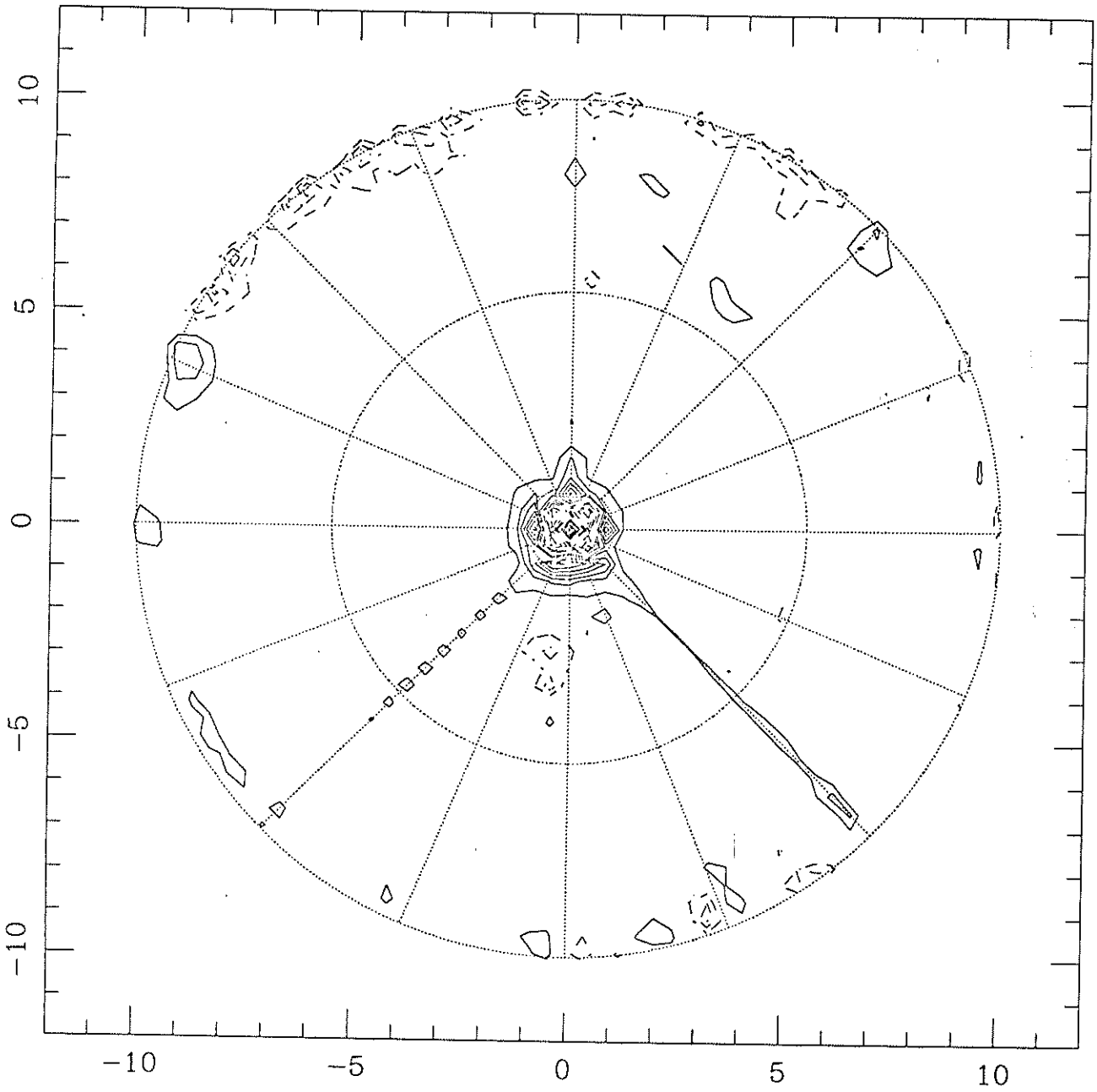

bmap31.242;12
ANTEN: 31

24-FEB-86
9:41 UT

IN/OUT FOCUS: 4105
UP/DWN FOCUS: 3721

CONTOURS:
−36.0 TO 36.0
INTERVAL 3.6

AFTER SUBTRACTING:
−0.11 −0.12 X +
0.23 Y +0.01 RSQ

RMS: 0.0018 INCHES

Figure 2. Aperture phase measured 24 Feb 1986, after final panel adjustment. Contours are the same as in Figure 1. The rms surface error is .0018 inches.

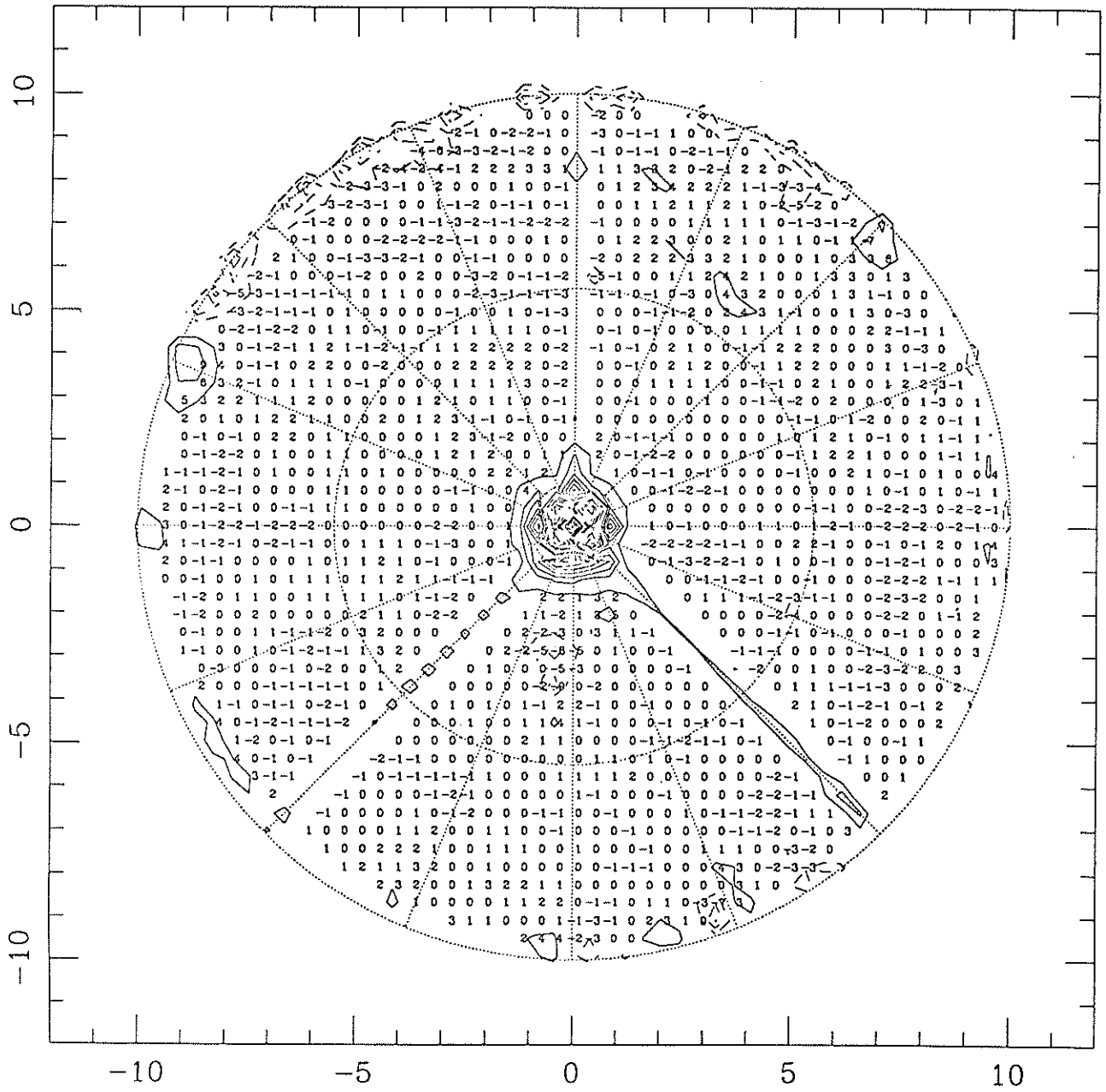

bmap31.242;12
ANTEN: 31

24−FEB−86
9:41 UT

IN/OUT FOCUS: 4105
UP/DWN FOCUS: 3721

CONTOURS:
−36.0 TO 36.0
INTERVAL 3.6

AFTER SUBTRACTING:
−0.11 −0.12 X +
0.23 Y +0.01 RSQ

RMS: 0.0018 INCHES

Figure 3. Same as figure 2, except the numbers used to calculate the rms are shown. Errors are in units of .001 inch. All points shown are independent. Data within 1 resolution element (5 inches) of the 3 feed legs, the central blockage, or the outer edge of the dish have been excluded in the rms calculation. All points are given equal weight in computing the rms error.

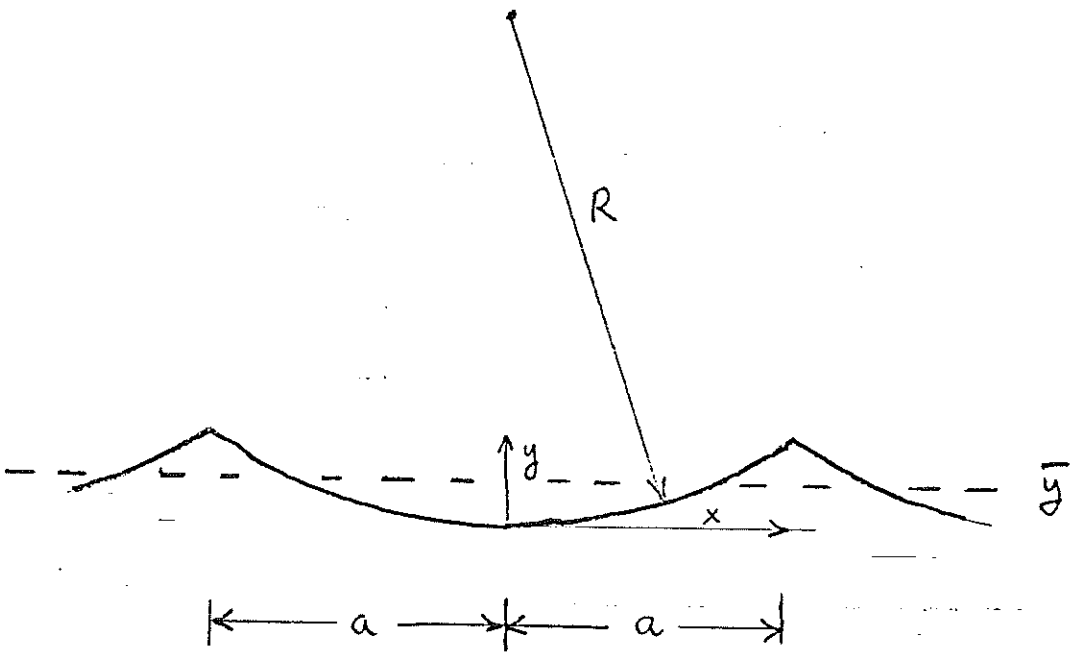

Figure 4. Calculation of rms surface error due to the machining marks left on the panels.

$$y(x) \approx \frac{1}{2}\frac{x^2}{R} \qquad \bar{y} = \frac{a^2}{6R}$$

$$\sigma^2 = \frac{1}{a}\int_0^a \left(\frac{1}{2}\frac{x^2}{R} - \frac{a^2}{6R}\right)^2 dx = \frac{1}{45}\frac{a^4}{R^2}$$

For antenna 3, R = 1 inch, 2a $\approx$ 0.15 inches, so $\sigma \approx$ 0.0008 inches.

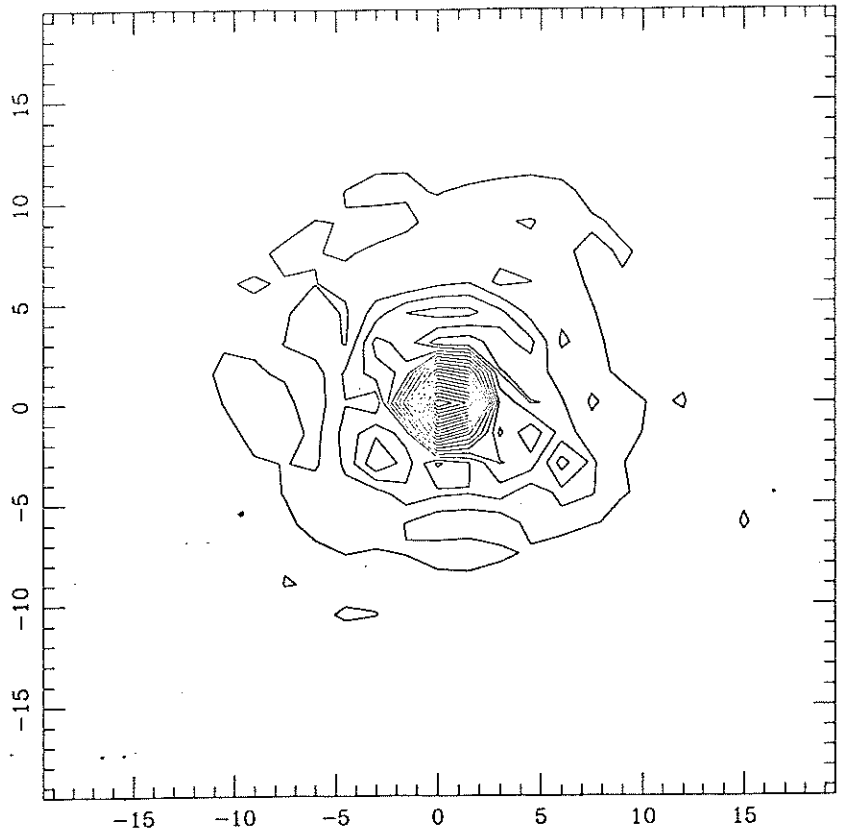

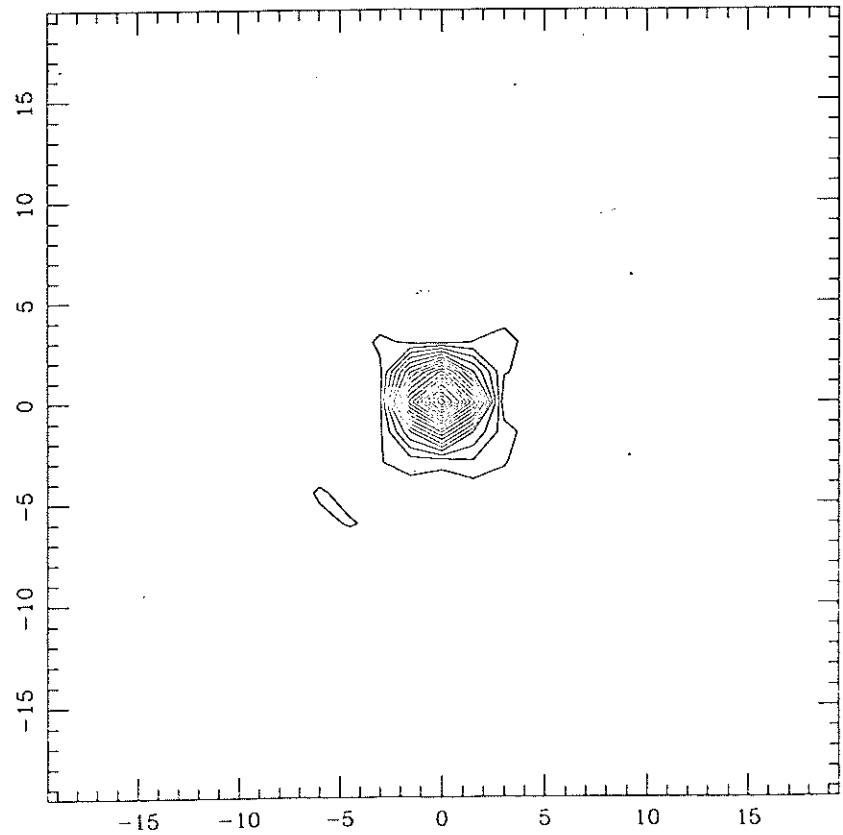

Figure 5. Antenna beam patterns measured before and after panel adjustment. Voltage contours are shown; the lowest contour is 5% of the peak, or -26 dB in power. The x- and y- axes are in arcminutes. The beam was sampled on a 1.5 arcminute grid.

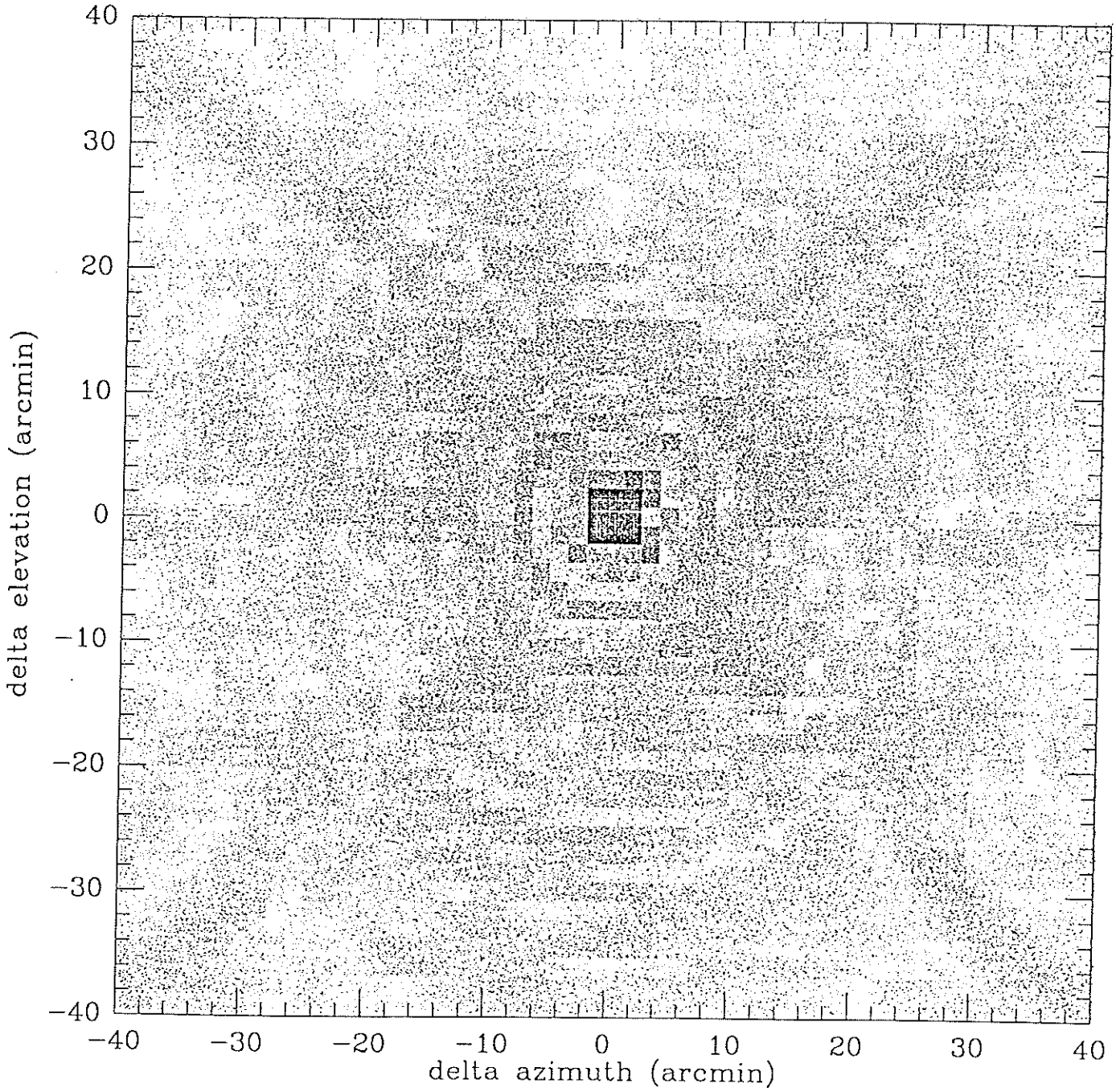

Figure 6. Halftone representation of the antenna beam pattern, extending over a square 80 arcminutes on a side. The gray scale ranges over beam voltages of 0–10% of the peak; thus, the scale represents structure in the power pattern at the levels of -20 dB to less than -40 dB. The faint horizontal and diagonal stripes (at about the -40 dB level) are caused by diffraction from the feed leg blockage.

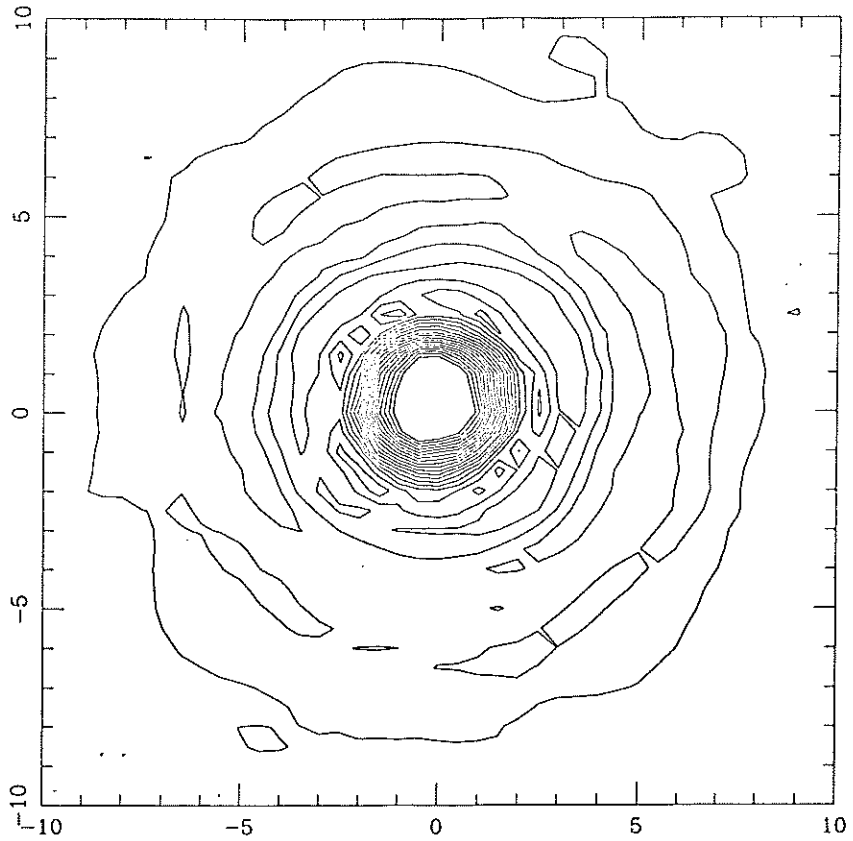

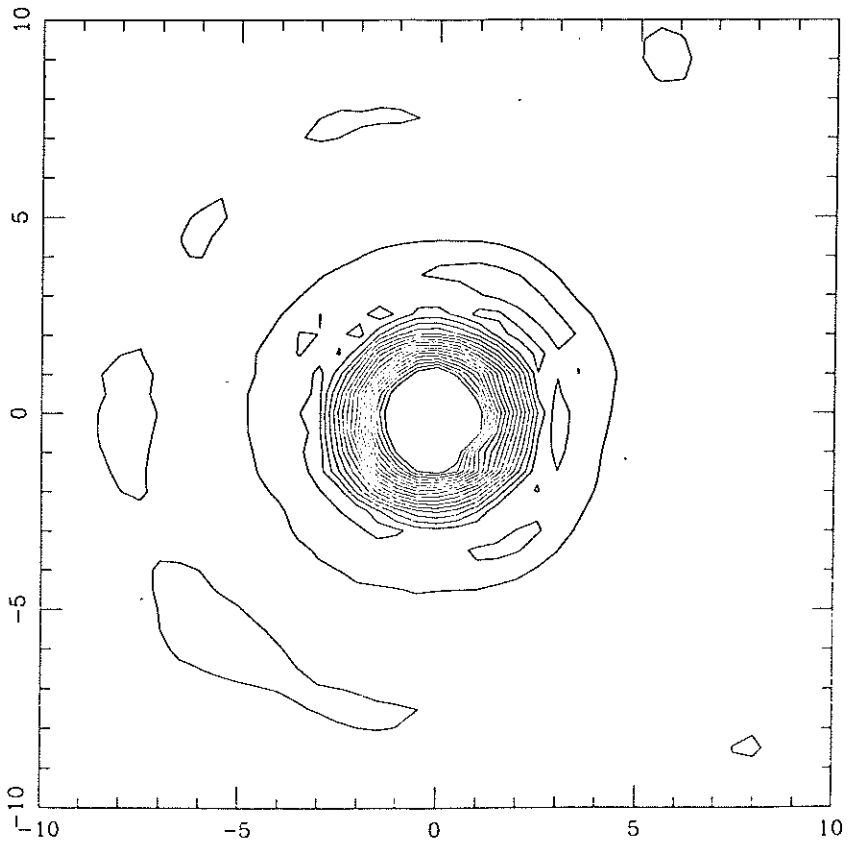

Figure 7. Antenna beam patterns with (*top*) and without (*bottom*) the Teflon lens installed, as measured with a 0.5 arcminute sampling interval on the remote transmitter. Contours are at 4% intervals in voltage, from 4% to 72% of the peak voltage. Thus, the innermost contour shown indicates the FWHM beamwidth; this is 2.2 arcminutes with the lens, 2.5 arcminutes without. As expected, the sidelobe level is higher with the lens installed.

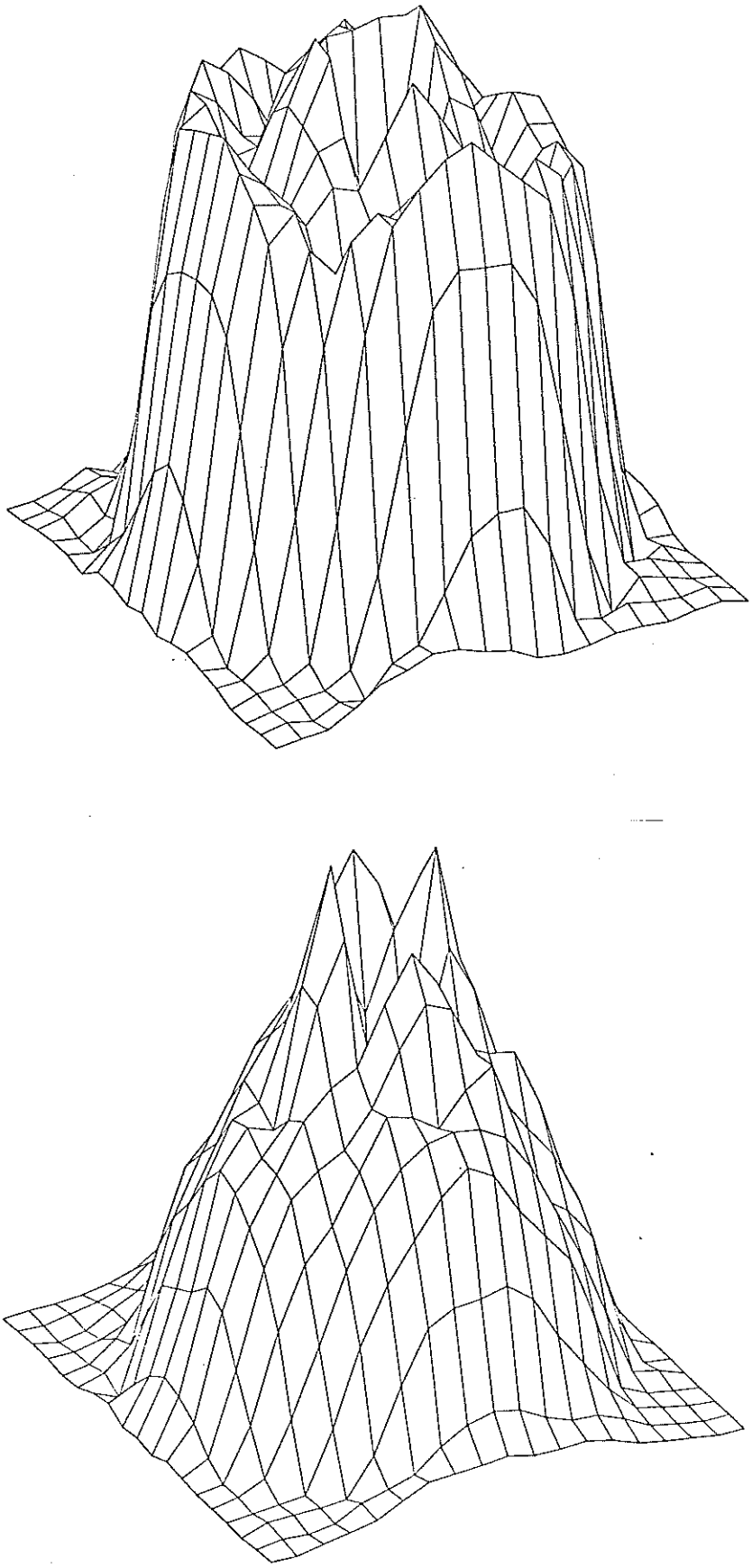

Figure 8. 3-dimensional representation of the electric field amplitude across the antenna aperture, measured with (*top*) and without (*bottom*) the Teflon lens installed. Blockage by the subreflector causes the hole at the center.

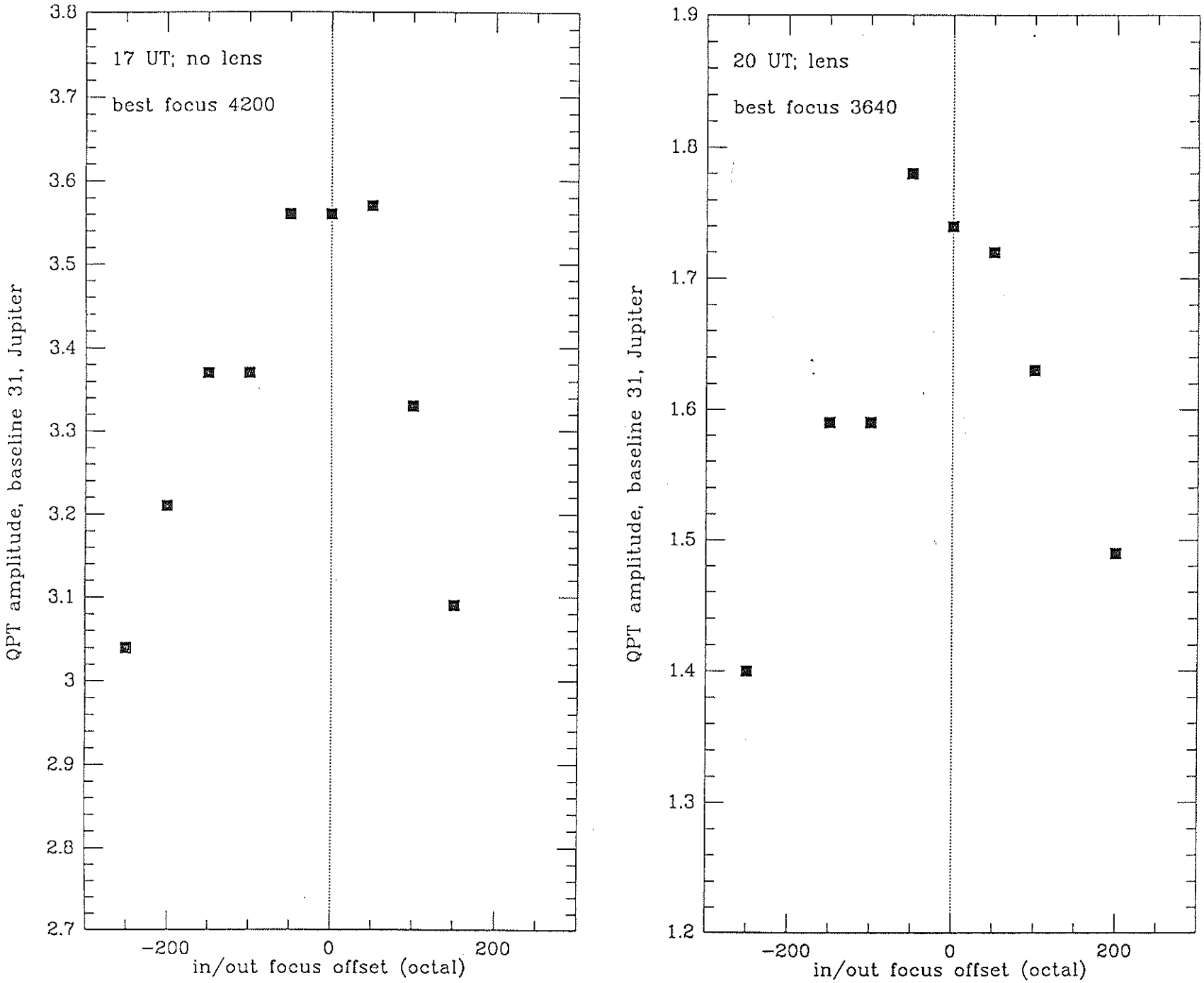

Figure 9. Focus curves obtained with program QPT. The focus was measured again without the lens at 23 UT, during the warmest part of the day, and was found to be 4040 at that time.

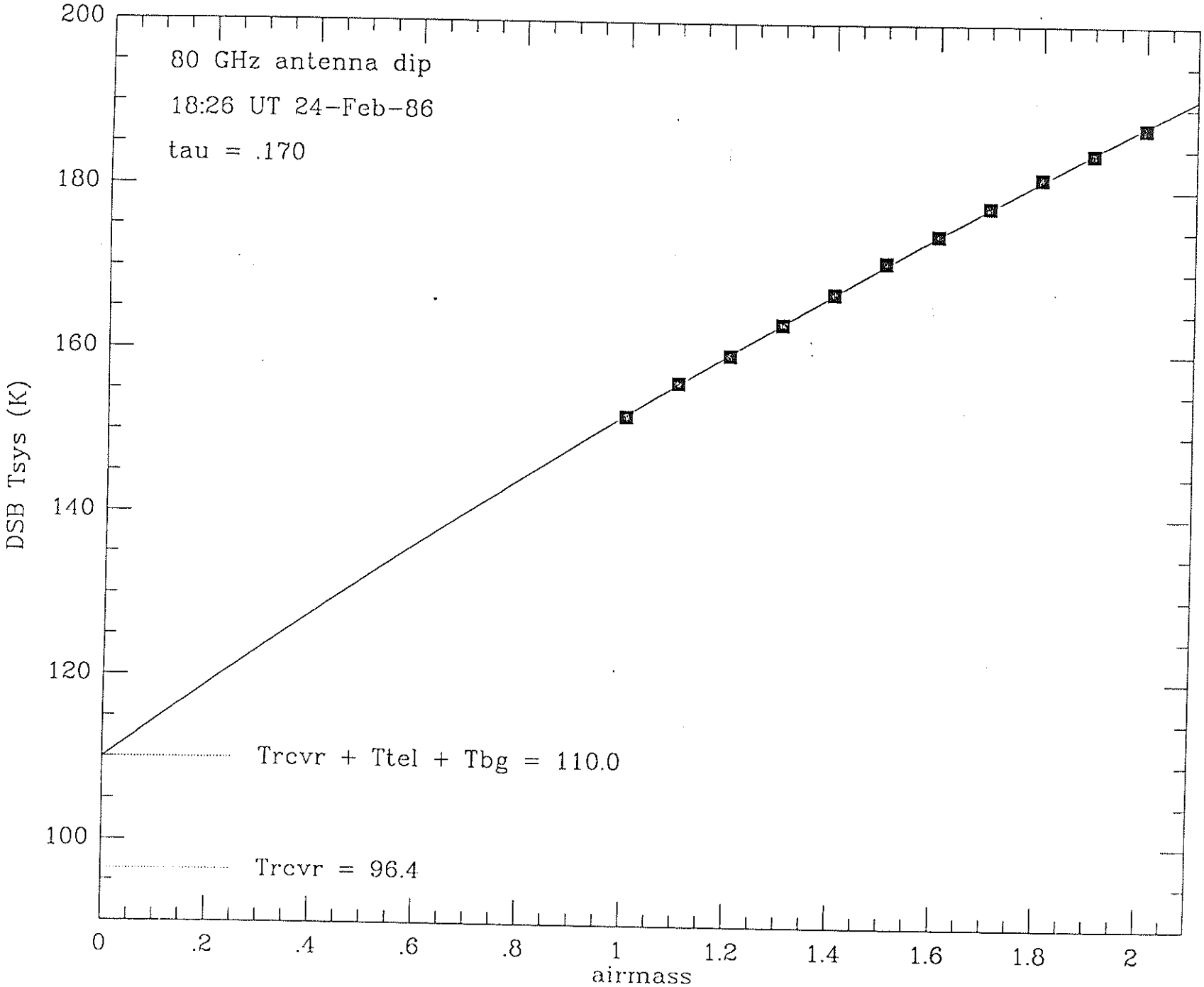

Figure 10. Antenna dipping curve at 80 GHz. Measured points are shown by squares; the smooth curve, showing the fit to the data, was generated by program [plambeck.apeff]dipfit.

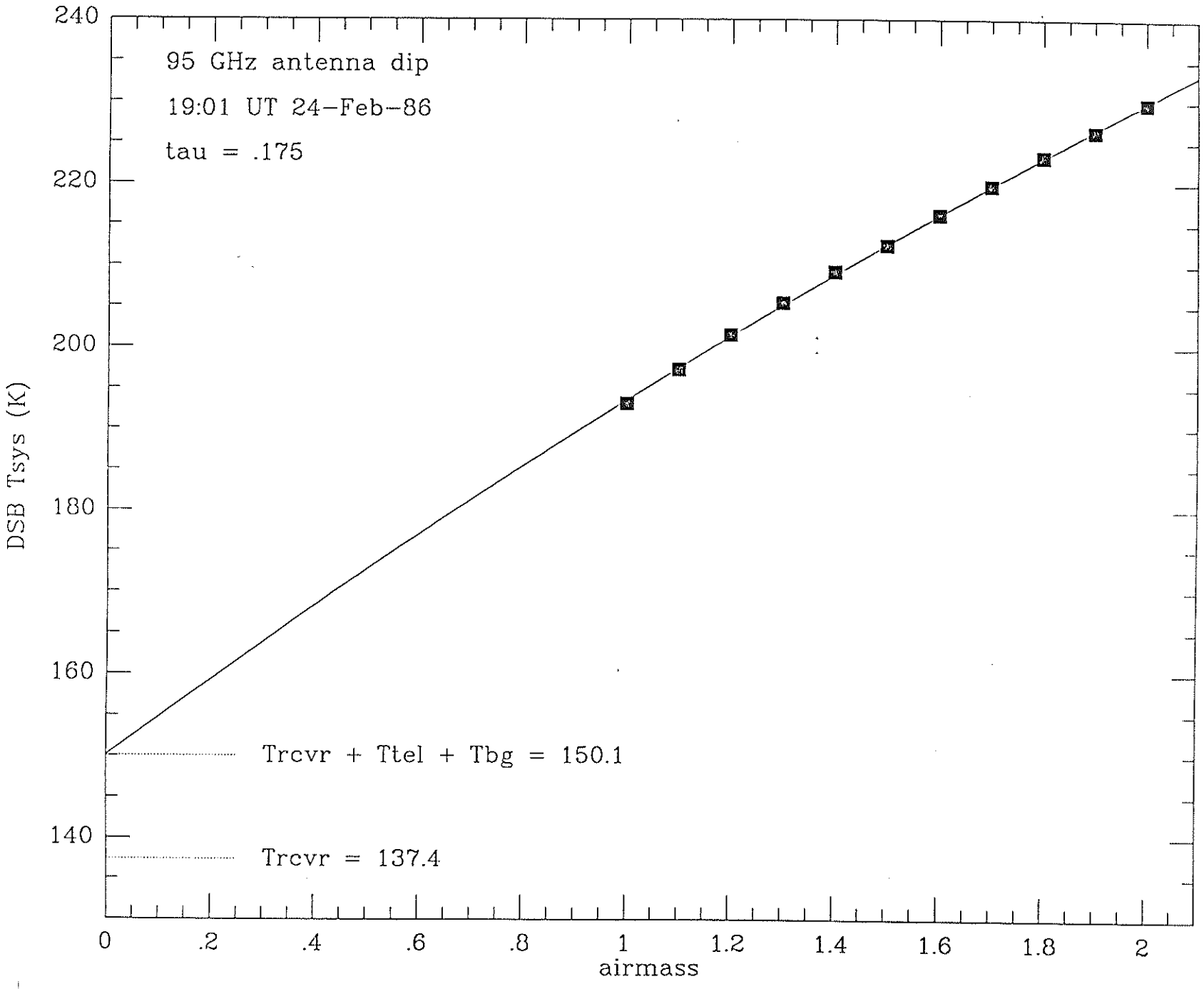

Figure 11. 95 GHz antenna dipping curve.

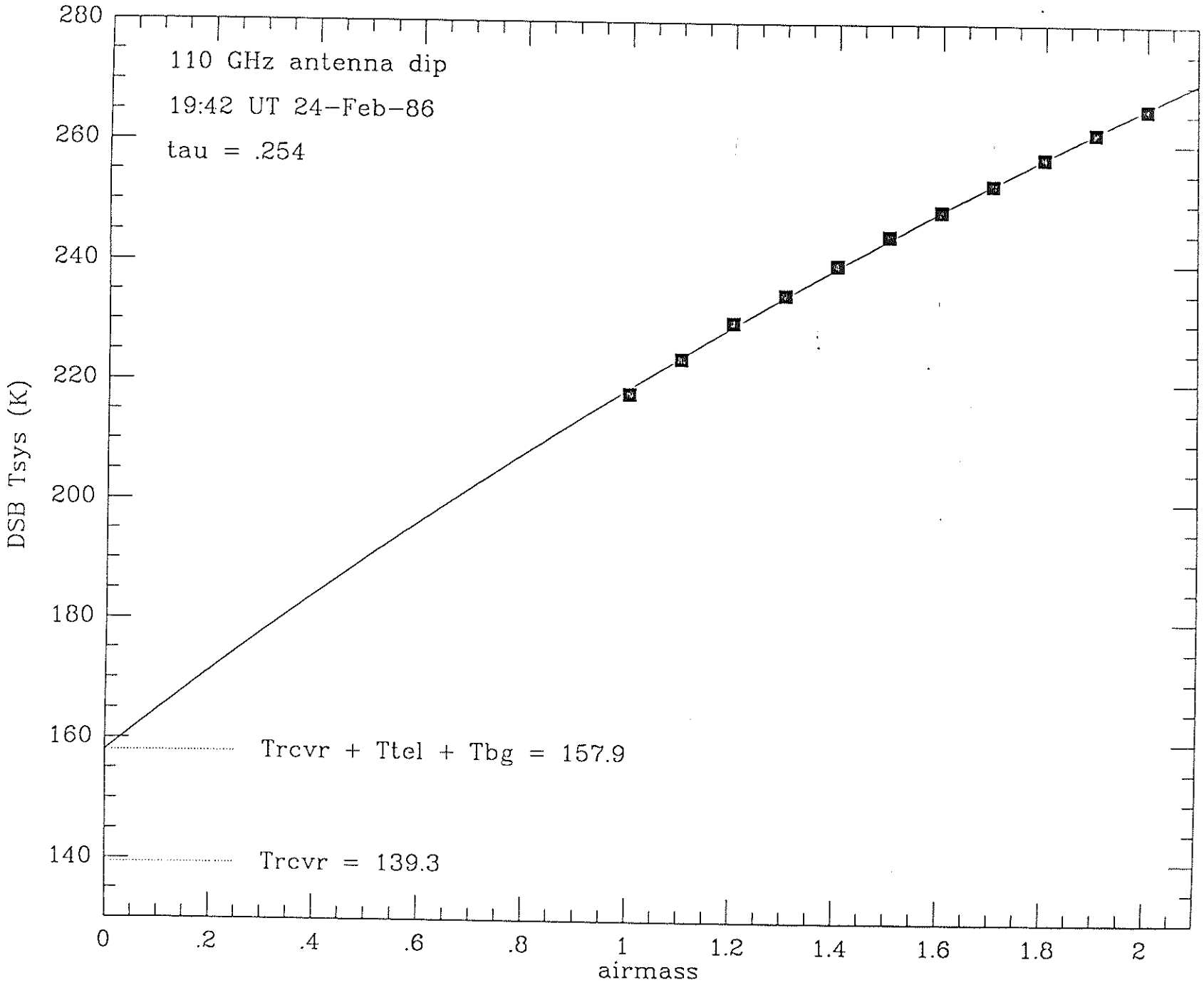

Figure 12. 110 GHz antenna dipping curve.

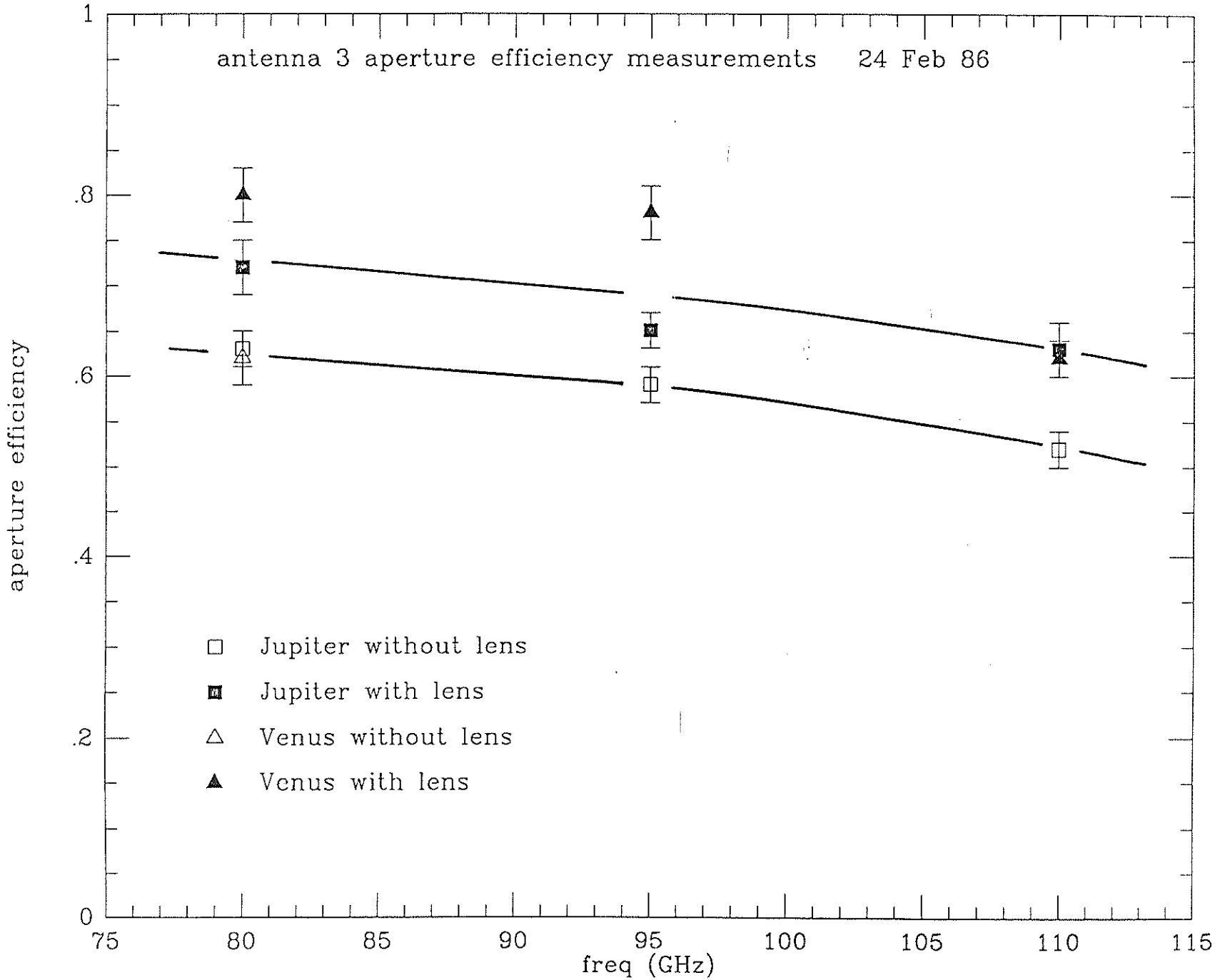

Figure 13. Measured aperture efficiency versus frequency. The dielectric lens appears to improve the efficiency by a factor of 15 to 20%.